# POTASSIUM CHANNELS SUPPORT ANION SECRETION IN PORCINE VAS DEFERENS EPITHELIAL CELLS

by

PRADEEP REDDY MALREDDY

B.V.Sc & A.H.
College of Veterinary Science,
Acharya N.G Ranga Agricultural University.
2001

A THESIS

submitted in partial fulfillment of the requirements for the degree

MASTER OF SCIENCE

Department of Anatomy and Physiology
College of Veterinary Medicine

KANSAS STATE UNIVERSITY
Manhattan, Kansas

2009

Approved by:

Major Professor

Bruce D. Schultz

# Abstract

Epithelial cells lining the vas deferens modify the luminal contents to which sperm are exposed in response to neuroendocrine, autocrine and lumicrine transmitters. The role and identity of vas deferens epithelial potassium channels that provide the correct luminal environment for sperm maturation and delivery have not yet been determined. Cultures of vas deferens epithelial cells isolated from adult pigs were employed to investigate contributions of selected ion channels to net flux. A two-pore potassium channel, TASK-2, was identified on the apical membrane of cultured primary porcine vas deferens epithelial cells (1°PVD). Bupivacaine, a known TASK-2 inhibitor, when added to the apical bathing solution, inhibited forskolin-stimulated short circuit current, $I_{sc}$, in a concentration dependent manner with a maximum inhibition of 72 ± 6% and an $IC_{50}$ of 7.4 ± 2.2 μM. Apical exposure of 1°PVD cells to quinidine, lidocaine, and clofilium (other known TASK-2 blockers) inhibited forskolin-stimulated $I_{sc}$ in a concentration dependent manner. Fitting a modified Michalis-Menten function to the data revealed $IC_{50}$ values of 274 μM, 531 μM, and 925 μM, respectively. Riluzole, a two-pore potassium channel activator, stimulated bupivacaine-sensitive $I_{sc}$, further confirming the contribution of TASK-2 to net ion flux. Western blotting demonstrated the presence of TASK-2 immunoreactivity in 1°PVD cell lysates, while immunocytochemistry demonstrated apical localization of the targeted epitope in virtually all cells lining native porcine vas deferens. These results suggest that TASK-2 likely plays a role in vas deferens epithelial ion transport that may account for the reportedly high concentration of potassium in the male reproductive duct lumen. TASK-2 likely contributes to male fertility as an integral member of the regulated transport processes that account for the luminal environment to which sperm are exposed.

# Table of Contents

# List of Figures

# List of Tables

# Acknowledgements

I thank my advisor and mentor **Dr. Bruce D Schultz** for all the guidance and support he has given me over last many years. He has helped me with some tough decisions for my career. I shall be very grateful for that. I extend my sincere gratitude to **Mr. Ryan Carlin** who taught me everything from the very basics of making solutions to conducting Ussing chamber experiments. I thank my fellow graduate students **Drs. Rebecca Quesnell** and **Suma Somasekharan** for their helpful nature and constructive criticism of my research endeavors. I thank **Terry O'Leary** for teaching me the basics of PCR. I thank **Dr. Fernando Alves** for having helpful discussions on almost anything related to work and life. I thank my fellow lab members **Florence Wang, Dr. Vladimir Akoyev, Cameron Duncan, Elizabeth Blaesi** and **Qian Wang** for creating pleasant work atmosphere. I thank **Dr. Daniel Marcus** for teaching me some of the basics of bioelectricity, letting me use the equipment in his laboratory and serving on my supervisory committee. I thank **Dr. Philine Wangemann** and **Joel Sanneman** for their help with confocal microscopy. I thank my other committee members, **Dr. Lisa Freeman** and **Dr. Larry Takemoto** for all their help. I am most thankful to **Drs. Walter Cash, Judy Klimek, Deryl Troyer** and **Jim Polikowski** for their help with teaching Gross Anatomy to freshmen DVM students. I thank **Dani, Bonnie,** and **Jenny** for their administrative support. I thank my friends **Dr. Bala Thiagarajan, Jessica Eichmiller, Nithya Raveendran, Dr. Satya Pondugula, Dr. Satish Medicetty** and **Dr. Raja Rachakatla** for their support and guidance. I thank all my friends here at K-State, **Sairam Jabba, Chanran Ganta, Kamesh, Kiran, Praveen,** and **Shiva.**

# Dedication

I dedicate this work to the late **Dr. Prakash Krishnaswami** and his wife **Sujatha Prakash** and my family.

# CHAPTER 1 - Introduction

## 1.1 Overview of $K^+$ Channels

Potassium channels are the most diverse group of proteins that are encoded by at least 100 different genes in humans alone (Hietzmann *et al*, 2008)(30). Potassium channels are expressed in almost all cell types including both excitable and non-excitable cells. All potassium channels share three basic properties: they have high conduction rates of about $10^7$ to $10^8$ ions per second, are selective for potassium ions and their conduction is gated (Doyle *et al*, 1998) (Fig. 1.1).

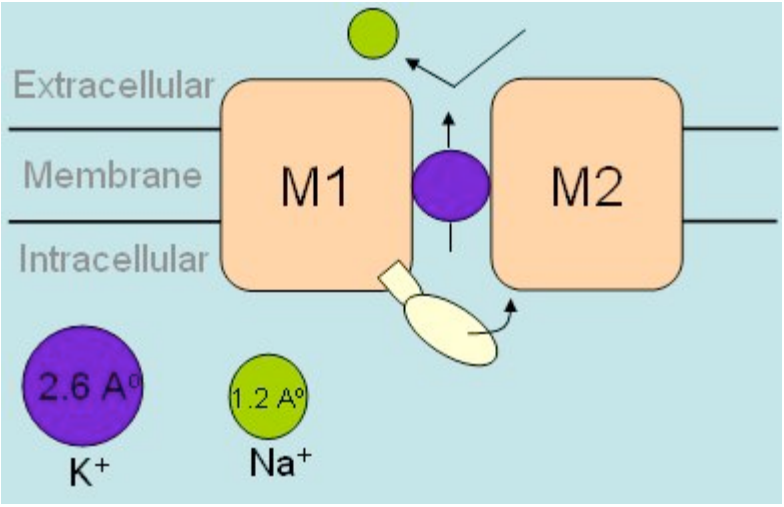


**Figure 1.1 Schematic diagram describing $K^+$ channel basic features.**

M1 and M2 represent transmembrane domains. The purple and green balls represent the relative dehydrated sizes of $K^+$ and $Na^+$ respectively. The $K^+$ is almost twice the size of $Na^+$. Yet $Na^+$, which is smaller, is essentially excluded as indicated by the green ball turning away from the pore. The conduction is turned on and off by opening and closing a gate, which can be regulated by an external stimulus such as ligand-binding or membrane voltage. (Fig. modified from Doyle *et al*, 1998).

The potassium channels present in non-excitable cells (e.g., epithelia) can be categorized broadly into three different groups based on structure: The first group is characterized by six transmembrane domains and one P-loop that is part of the ion-conducting pore (6TMD/1P, Fig. 1.2A), which includes voltage-dependent ($K_v$) and calcium-activated ($K_{Ca}$) $K^+$ channels. $K_v$ channels are gated by membrane voltage, i.e., they open and close in response to changes in membrane potential. $K_v$ channels comprise a large group of $K^+$ channels encoded by at least 40 different genes in humans (Gutman *et al*, 2003 and 2005) and are preferentially expressed in excitable cells. $K_v$ channels expressed in non-excitable cell types such as renal (Hebert *et al*, 2003), gastro-intestinal (Hietzmann *et al*, 2008) and respiratory epithelia (Bardou *et al*, 2009) have an essential role in various functions including electrolyte and substrate transport, cell volume regulation, cell migration, wound healing, proliferation, apoptosis, carcinogenesis, and oxygen sensing (O'Grady *et al*, 2005). $K_{Ca}$ channels are gated by intracellular $Ca^{2+}$ concentration. $Ca^{2+}$ may interact directly with the channel protein or may cause a secondary signaling cascade that may then either activate or inhibit the channel. $K_{Ca}$ channels have been studied extensively in the nervous system where they play an important role in regulation of intracellular $Ca^{2+}$ concentration. $K_{Ca}$ in epithelial cell types have been shown to play an important role in $O_2$ sensing in alveoli (Jovanovic *et al*, 2003), kidney cell migration (Schwab *et al*, 2001), inflammatory responses in lung pathologies (Dulong *et al*, 2007) and control of $Cl^-$ secretion in airways (Devor *et al*, 2000; Cowley *et al*, 2002; Bernard *et al*, 2003)

The second group is characterized by two TMD and one P-loop (2TMD/1P, Fig. 1.2C), which includes inward-rectifier $K^+$ channels (Kir) (Bardou *et al*, 2009). A functional Kir channel like Kv channels, is believed to be a tetramer. However, a striking biophysical property of these

channels is the inward rectification, which refers to greater $K^+$ conductance under hyperpolarization and lesser conductance under depolarization, the effect opposite to that seen in $K_v$ channels (Lu, 2004). These $K^+$ channels are involved in repolarization of action potentials, setting the resting potential of the cell and contributing to $K^+$ homeostasis. Gene mutations of inward rectifiers have been linked to several human diseases including Bartter syndrome (Simon *et al*, 1996) and Andersen's syndrome (Plaster *et al*, 2001).

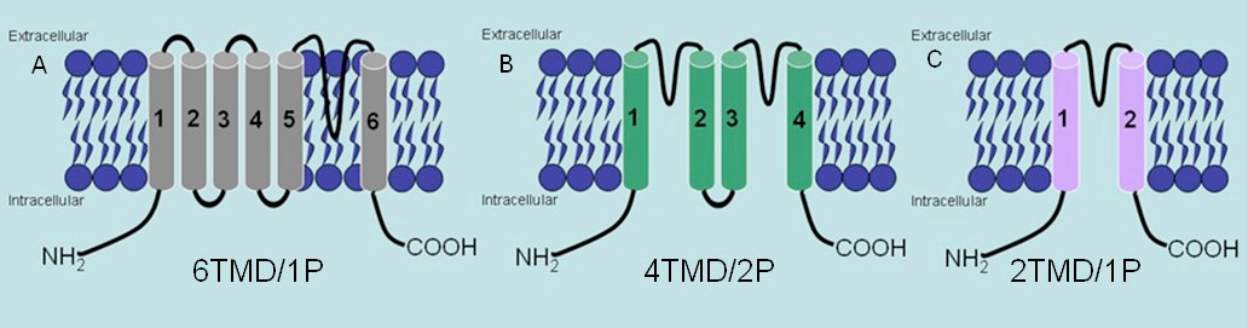


**Figure 1.2 Topology of $K^+$ channel α-subunits.**

The numbers (1-6) represent the transmembrane segments. A, B, C) Each panel represents an α-subunit of a well-described class of $K^+$ channels. A, C) A functional $K^+$ channel is formed by the homo- or hetero-tetramerization of subunits. B) A functional $K_{2P}$ channel is formed by the dimerization of 4TMD/2P sub-units. (Modified from Bardou *et al*, 2009).

The third group is characterized by four TMD and two P-loops (4TMD/2P, Fig. 1.2B), which includes two-pore $K^+$ channels ($K_{2P}$) (Lesage et al, 2000). The first member of the two-pore $K^+$ channel family was named TWIK-1 for Tandem of P domains in a Weak Inward Rectifying $K^+$ channel. Currently, fifteen mammalian genes have been identified that code for $K_{2P}$ family members. $K_{2P}$ channels are further classified in to six subfamilies based on their functional domains and include TWIK, TREK, TASK, TALK, THIK and TRESK. $K_{2P}$ $K^+$

channels are expressed in a number of different cell types and have distinct functions depending on the channel subtype expressed.

## 1.2 TASK Channels

TWIK related Acid Sensitive $K^+$ (TASK) channels are expressed in many tissues and cell types including the brain, heart, lung, kidney, small intestine, liver, pancreas, placenta and testis (Reyes *et al*, 1998). TASK channels are constitutively active near resting membrane potential (Duprat *et al*, 1997) and thus were also referred to as background or leak channels. The TASK channel family is comprised of five different isoforms: TASK-1, TASK-2, TASK-3, TASK-4, and TASK-5. All these isoforms are sensitive to extracellular pH, which makes them strong candidates for the $K^+$ conductance(s) contributing to, or regulating pH-sensitive ion transport systems. For example in murine kidney proximal tubules, TASK-2 channels are activated by an increase in luminal pH due to bicarbonate transport (Warth *et al*, 2004). TASK-2 is also involved in the regulation of apoptosis in kidney proximal tubule cells. Apoptosis in TASK-2 knock out mice was significantly reduced suggesting a role in apoptotic volume decrease in kidney proximal tubule cells (L'Hoste *et al*, 2007a). TASK channels are known to be involved in neuronal protection (Liu *et al*, 2005) and general anesthesia (Patel *et al*, 1999). Expression of TASK channels in hippocampal cells resulted in a significant protection from an oxygen-glucose deprivation injury and this neuroprotection was enhanced in the presence of isoflurane, a general anesthetic (Liu *et al* 2005). Involvement of TASK-2 has been suggested in volume regulation of spermatozoa in mice (Barfield *et al*, 2005). It is known that spermatozoa have high $K^+$ concentration (Chou *et al*, 1989) and that $K^+$ concentration increases in luminal fluids along the

length of epididymis and vas deferens (Turner *et al*, 2002). Hence a role for TASK-2 in the vas deferens is plausible.

## 1.3 Identification of TASK-2 $K^+$ Channels

Pharmacological agents that selectively either block or activate an ion channel have been employed to implicate contributions of distinct channels to overall tissue functions. Of the wide range of $K^+$ channel blockers available, tetraethyl ammonium (TEA), 4-aminopyridine (4-AP), $Cs^+$, and $Ba^{2+}$ have been used as broad-spectrum $K^+$ channel blockers. However, $K_{2P}$ channels are relatively insensitive to these $K^+$ channel blockers.

Local anesthetics including bupivacaine and lidocaine inhibit TASK-2 in heterologously expressed cells in a concentration dependent manner. These local anesthetics are also known to inhibit other $K_{2P}$ channels including TASK-1 and TASK-3 and voltage-gated $Na^+$ channels. The concentration required to inhibit conductance by 50% ($IC_{50}$) for TASK-2 inhibition by bupivacaine in HEK293 cells is in the low to mid-micro molar range (17 μM; Kindler *et al*, 2003), and the $IC_{50}$ for inhibition of voltage-gated $Na^+$ channels in HEK293 cells is in the same range (4.5 μM; Wang *et al*, 2001). The effects of quinine and quinidine on currents elicited by voltage pulses to +50 mV have been studied in TASK-2-expressing COS cells. Quinidine, at 100 μM, induced a 65 ± 3.8% inhibition of the current in these cells (Reyes *et al*, 1999). It has been reported that clofilium inhibited $K^+$ currents in mTASK-2-transfected HEK293 cells in a concentration dependent manner (Niemeyer *et al*, 2001) with an $IC_{50}$ of ~25 μM. Thus bupivacaine, lidocaine, quinidine, and clofilium can provide pharmacological profile to characterize TASK-2 $K^+$ channel currents.

Riluzole reportedly activates TASK-2 channels in Calu-3 cells, a cell line derived from human airway (11), an attribute that makes it potentially valuable for the proposed studies. However this compound has been shown also to activate TREK-1 and TRAAK, two members of $K_{2P}$ family that are closely related to TASK-2 and riluzole has been shown to affect other classes of ion channels. For example riluzole was shown to activate small conductance, $Ca^{2+}$-activated $K^+$ channels (SK channels) expressed HEK293 cells (Cao *et al*, 2002). These activities of riluzole across classes of ion channels greatly diminish the diagnostic value of the drug. Nonetheless, riluzole can be used as one component in a pharmacological toolbox that is assembled to either implicate or exclude a contribution of TASK-2 to the physiological function of a tissue.

The selection of $K_{2P}$ channels in general and TASK-2 channels specifically as a focus point for the proposed studies was built on a limited amount of preliminary information. Specifically, microarray analysis of RNA isolated from human vas deferens epithelial cells revealed message coding for various $K^+$ channels including $K_{2P}$ channels (Table 1). Ultimately, experiments were conducted employing cells and tissues isolated from pigs because of their availability. Outcomes of initial experiments guided the research to focus on TASK-2.

**Table 1.1 Candidate genes for $K^+$ conductance in human vas deferens epithelial cells.**

| $K_{Ca}$ | $K_v$ | Kir | $K_{2P}$ |
|---|---|---|---|
| KCNN4 (SK4) | KCNC4 (Kv3.4) | KCNJ15 (Kir1.3) | KCNK1 (TWIK1) |
| KCNMB4 (MaxiK) | KCND1 (Kv4.1) | KCNJ2 (Kir2.1) | KCNK6 (TWIK2) |
| | KCNQ1 (Kv7.1) | KCNJ16 (Kir5.1) | KCNK3 (TASK1) |
| | KCNQ3 (Kv7.3) | KCNJ3 (GIRK) | **KCNK5 (TASK2)** |
| | KCNS1 (Kv9.1) | | KCNK17 (TASK4) |
| | KCNS3 (Kv9.3) | | KCNK10 (TREK2) |

## 1.4 References


Bardou O, Trinh NT, and Brochiero E. Molecular diversity and function of $K^+$ channels in airway and alveolar epithelial cells. Am J Physiol Lung Cell Mol Physiol 296: L145-155, 2009.

Barfield JP, Yeung CH, and Cooper TG. The effects of putative $K^+$ channel blockers on volume regulation of murine spermatozoa. Biol Reprod 72: 1275-1281, 2005.

Bernard K, Bogliolo S, Soriani O, and Ehrenfeld J. Modulation of calcium-dependent chloride secretion by basolateral SK4-like channels in a human bronchial cell line. J Membr Biol 196: 15-31, 2003.

Chou K, Chen J, Yuan SX, and Haug A. The membrane potential changes polarity during capacitation of murine epididymal sperm. Biochem Biophys Res Commun 165: 58-64, 1989.

Cowley EA and Linsdell P. Characterization of basolateral $K^+$ channels underlying anion secretion in the human airway cell line Calu-3. J Physiol 538: 747-757, 2002.

Doyle DA, Morais Cabral J, Pfuetzner RA, Kuo A, Gulbis JM, Cohen SL, Chait BT, and MacKinnon R. The structure of the potassium channel: molecular basis of $K^+$ conduction and selectivity. Science 280: 69-77, 1998.

Dulong S, Bernard K, and Ehrenfeld J. Enhancement of P2Y6-induced Cl- secretion by IL-13 and modulation of SK4 channels activity in human bronchial cells. Cell Physiol Biochem 20: 483-494, 2007.

Duprat F, Lesage F, Fink M, Reyes R, Heurteaux C, and Lazdunski M. TASK, a human background $K^+$ channel to sense external pH variations near physiological pH. EMBO J 16: 5464-5471, 1997.

Gutman GA, Chandy KG, Adelman JP, Aiyar J, Bayliss DA, Clapham DE, Covarriubias M, Desir GV, Furuichi K, Ganetzky B, Garcia ML, Grissmer S, Jan LY, Karschin A, Kim D, Kuperschmidt S, Kurachi Y, Lazdunski M, Lesage F, Lester HA, McKinnon D, Nichols CG, O'Kelly I, Robbins J, Robertson GA, Rudy B, Sanguinetti M, Seino S, Stuehmer W, Tamkun MM, Vandenberg CA, Wei A, Wulff H, and Wymore RS. International Union of Pharmacology.

XLI. Compendium of voltage-gated ion channels: potassium channels. Pharmacol Rev 55: 583-586, 2003.

Gutman GA, Chandy KG, Grissmer S, Lazdunski M, McKinnon D, Pardo LA, Robertson GA, Rudy B, Sanguinetti MC, Stuhmer W, and Wang X. International Union of Pharmacology. LIII. Nomenclature and molecular relationships of voltage-gated potassium channels. Pharmacol Rev 57: 473-508, 2005.

Hebert SC, Desir G, Giebisch G, and Wang W. Molecular diversity and regulation of renal potassium channels. Physiol Rev 85: 319-371, 2005.

Heitzmann D and Warth R. Physiology and pathophysiology of potassium channels in gastrointestinal epithelia. Physiol Rev 88: 1119-1182, 2008.

Jovanovic S, Crawford RM, Ranki HJ, and Jovanovic A. Large conductance $Ca^{2+}$-activated $K^{+}$ channels sense acute changes in oxygen tension in alveolar epithelial cells. Am J Respir Cell Mol Biol 28: 363-372, 2003.

L'Hoste S, Poet M, Duranton C, Belfodil R, e Barriere H, Rubera I, Tauc M, Poujeol C, Barhanin J, and Poujeol P. Role of TASK2 in the control of apoptotic volume decrease in proximal kidney cells. J Biol Chem 282: 36692-36703, 2007.

Liu C, Cotten JF, Schuyler JA, Fahlman CS, Au JD, Bickler PE, and Yost CS. Protective effects of TASK-3 (KCNK9) and related 2P K channels during cellular stress. Brain Res 1031: 164-173, 2005.

Lu Z. Mechanism of rectification in inward-rectifier $K^+$ channels. Annu Rev Physiol 66: 103-129, 2004.

Miller C. An overview of the potassium channel family. Genome Biol 1: REVIEWS0004, 2000.

O'Grady SM and Lee SY. Molecular diversity and function of voltage-gated (Kv) potassium channels in epithelial cells. Int J Biochem Cell Biol 37: 1578-1594, 2005.

Patel AJ, Honore E, Lesage F, Fink M, Romey G, and Lazdunski M. Inhalational anesthetics activate two-pore-domain background $K^+$ channels. Nat Neurosci 2: 422-426, 1999.

Plaster NM, Tawil R, Tristani-Firouzi M, Canun S, Bendahhou S, Tsunoda A, Donaldson MR, Iannaccone ST, Brunt E, Barohn R, Clark J, Deymeer F, George AL, Jr., Fish FA, Hahn A, Nitu A, Ozdemir C, Serdaroglu P, Subramony SH, Wolfe G, Fu YH, and Ptacek LJ. Mutations in Kir2.1 cause the developmental and episodic electrical phenotypes of Andersen's syndrome. Cell 105: 511-519, 2001.

Reyes R, Duprat F, Lesage F, Fink M, Salinas M, Farman N, and Lazdunski M. Cloning and expression of a novel pH-sensitive two pore domain K+ channel from human kidney. J Biol Chem 273: 30863-30869, 1998.

Schwab A. Ion channels and transporters on the move. News Physiol Sci 16: 29-33, 2001.

Simon DB and Lifton RP. The molecular basis of inherited hypokalemic alkalosis: Bartter's and Gitelman's syndromes. Am J Physiol 271: F961-966, 1996.

Singh AK, Devor DC, Gerlach AC, Gondor M, Pilewski JM, and Bridges RJ. Stimulation of $Cl^-$ secretion by chlorzoxazone. J Pharmacol Exp Ther 292: 778-787, 2000.

Warth R, Barriere H, Meneton P, Bloch M, Thomas J, Tauc M, Heitzmann D, Romeo E, Verrey F, Mengual R, Guy N, Bendahhou S, Lesage F, Poujeol P, and Barhanin J. Proximal renal tubular acidosis in TASK2 $K^+$ channel-deficient mice reveals a mechanism for stabilizing bicarbonate transport. Proc Natl Acad Sci U S A 101: 8215-8220, 2004

# CHAPTER 2 - TASK-2 potassium channel supports ion secretion in pig vas deferens epithelia

Pradeep R. Malreddy and Bruce D. Schultz

Department of Anatomy & Physiology, Kansas State University, Manhattan, KS 66506

**This chapter has been submitted in this format for review to a peer reviewed journal.**

## 2.1 Abstract

Epithelial cells lining the vas deferens modify the luminal contents to which sperm are exposed in response to neuroendocrine, autocrine and lumicrine transmitters. The role and identity of vas deferens epithelial potassium channels that provide the correct luminal environment for sperm maturation and delivery have not yet been determined. Cultures of vas deferens epithelial cells isolated from adult pigs were employed to investigate contributions of selected ion channels to net flux. A two-pore potassium channel, TASK-2, was identified on the apical membrane of cultured primary porcine vas deferens epithelial cells (1°PVD). Bupivacaine, a known TASK-2 inhibitor, when added to the apical bathing solution, inhibited forskolin-stimulated short circuit current, $I_{sc}$, in a concentration dependent manner with a maximum inhibition of 72 ± 6% and an $IC_{50}$ of 7.4 ± 2.2 μM. Apical exposure of 1°PVD cells to quinidine, lidocaine, and clofilium (other known TASK-2 blockers) inhibited forskolin-stimulated $I_{sc}$ in a concentration dependent manner. Fitting a modified Michalis-Menten function to the data revealed $IC_{50}$ values of 274 μM, 531 μM, and 925 μM, respectively. Riluzole, a two-pore potassium channel activator, stimulated bupivacaine-sensitive $I_{sc}$, further confirming the contribution of TASK-2 to net ion flux. Western blotting demonstrated the presence of TASK-2 immunoreactivity in 1°PVD cell lysates, while immunocytochemistry demonstrated apical localization of the targeted epitope in virtually all cells lining native porcine vas deferens. These results suggest that TASK-2 likely plays a role in vas deferens epithelial ion transport that may account for the reportedly high concentration of potassium in the male reproductive duct lumen. TASK-2 likely contributes to male fertility as an integral member of the regulated transport processes that account for the luminal environment to which sperm are exposed.

## 2.2 Introduction

Vas deferens historically have been considered to be conduits for the transportation of sperm and as a storage organ until ejaculation. Many studies have evaluated the fluid transport across rete testis, efferent ducts and epididymis but none have evaluated the vas deferens (8, 20, 43). Nonetheless, the vas deferens functions to provide the correct luminal environment for sperm maturation. Epithelium lining the vas deferens likely plays a major role in determining the composition of the luminal fluids to which sperm are exposed. Initial studies in rat male reproductive tract luminal fluid volume changes suggest the absorptive nature of the epithelia lining the male reproductive tract with ~50% of reabsorption of fluids taking place between seminiferous tubules and the caput epididymis and 50% of the remaining fluid reabsorption between the caput and the vas deferens (26). More recent studies have shown that these epithelia are capable of anion secretion in response to various neurotransmitters (4, 35), neuro-hypophyseal hormones (18), and autacoids (33) at physiological concentrations. For electrogenic anion secretion to occur, one or more basolateral $K^+$ channels are likely required, along with other ion transport mechanisms (37). However, there are reports demonstrating the presence of apical $K^+$ channels in certain anion-secreting epithelia including cells lining the epididymis (9), lacrimal acinar cells (39), and Calu-3 cells, an epithelial cell line derived from human airway (11). The concept of $K^+$ channels on the apical membrane and their contribution in supporting the anionic secretion is an emerging field.

The $K^+$ concentration in the luminal fluid of vas deferens of rat (26), ram, boar, bull (10), and hamster (40), and man (19) is high relative to the plasma concentration. This may be

attributable to three causes: 1) Selective absorption of water and other solutes in the seminiferous tubules, epididymes (8), and perhaps vas deferens 2) Secretion of $K^+$ by spermatozoa, and 3) Secretion of $K^+$ by epithelial cells lining the lumen of epididymis and vas deferens (38). Human vas deferens epithelial cells reportedly have maxi $K^+$ channel activity in the apical membranes (38). Also, high $K^+$ concentration in the rat caudal epididymal fluid has been shown to inhibit initiation of sperm motility (42). Hence, it was speculated that $K^+$ channels are located on the apical plasma membrane of porcine vas deferens epithelial cells and could provide a pathway for $K^+$ secretion at this location. The luminal environment of vas deferens can be either acidic or alkaline in nature depending upon the activity of proton and bicarbonate secreting mechanisms (3, 5, 6). Thus, it seems logical that an acid-sensitive $K^+$ channel might be present on the apical membrane of the porcine vas deferens epithelial cells to account for regulated $K^+$ secretion.

Two-pore $K^+$ channels ($K_{2P}$) are characterized by four transmembrane segments and two pore domains as opposed to the usual one pore domains that are found in other $K^+$ channel families. The first member of the two-pore $K^+$ channel family was named TWIK-1 for Tandem of P domains in a Weak Inward Rectifying $K^+$ channel (24, 25). Two-pore $K^+$ channels have been shown to be expressed in a number of different cell types since their discovery about twelve years ago. Currently, fifteen mammalian genes have been identified that code for two-pore $K^+$ channel family members. These channels have been grouped into different two-pore $K^+$ channel families based on their respective functional properties (17, 25). One of them is the TWIK-related Acid-Sensitive $K^+$ channel (TASK) family. The TASK channel family has five different members. These channels are all sensitive to the extracellular pH (2, 12, 14, 21, 34) and exhibit modest sequence homology (17). TASK-2 is a unique two-pore $K^+$ channel with high sensitivity

to external pH in the physiological range and wide tissue distribution. TASK-2 mRNA is expressed in various epithelial tissues including uterus, ovary, testis, kidney, lung, stomach, intestine, colon, and salivary gland (34), but is poorly expressed or absent in excitable tissues like brain and muscle (34). Whether TASK-2 or any other two-pore channel is present in porcine vas deferens epithelial cells is not known.

The goal of this study was to determine whether TASK-2 $K^+$ channels have a role in modulating epithelial ion transport across porcine vas deferens epithelia. A two-pronged approach was employed in which cultured cells were either placed in modified Ussing flux chambers to test for effects on ion transport by known TASK-2 modulators or the cells were lysed to probe protein samples with anti-TASK-2 antibodies. Finally, immunohistochemistry was employed to provide evidence for the presence of TASK-2 on the apical membrane of epithelial cells lining freshly isolated vas deferens.

## 2.3 Materials and Methods

### *2.3.1 Culture of Porcine Vas Deferens Epithelial Cells (1°PVD Cells)*

Methods for isolation and culture of porcine vas deferens epithelial cells were reported in detail previously (35). Briefly, adult male reproductive tracts were obtained from a local slaughter house and maintained in ice-cold Ringer solution (composition in mM: 120 NaCl, 25 $NaHCO_3$, 3.3 $KH_2PO_4$, 0.83 $K_2HPO_4$, 1.2 $CaCl_2$, and 1.2 $MgCl_2$) until further processing at the laboratory. Those portions of the deferent ducts that extend from the transitional epididymis/vas deferens to the prostate gland were used to isolate epithelial cells. Ducts were

flushed with a collagenase-based dissociation solution to obtain the epithelial cells that then were seeded onto tissue culture flasks. Cells were incubated at 37°C at 5% $CO_2$ in Dulbecco modified Eagle medium (DMEM; GIBCO-BRL, Grand Island, NY) supplemented with 10% fetal bovine serum (FBS; HyClone, Logan, UT) and 1% penicillin and streptomycin (Invitrogen, Carlsbad, CA). The cells were allowed to grow to confluence (about 3-4 days) and then were subcultured onto Snapwell permeable supports (1.13 $cm^2$, Costar, Cambridge, MA). The media on both basolateral and apical sides were changed the day following subculture and every other day thereafter until assays were performed, typically 14 days after seeding.

*2.3.2 Electrophysiology*

Transepithelial electrical resistance ($R_{te}$), transepithelial potential difference ($PD_{te}$), basal short-circuit current ($I_{sc}$) and changes in $I_{sc}$ stimulated/inhibited by select pharmacological agents across 1°PVD monolayers on Snapwell permeable supports were assessed using a modified Ussing chamber apparatus (Model DCV9, Navicyte, San Diego, CA). The experiments were conducted in symmetrical Ringer solution at 39°C with continuous bubbling of 5% $CO_2$ and 95% $O_2$. The monolayers were clamped to zero $PD_{te}$ using a voltage clamp apparatus (Model 558C, University of Iowa, Department of Bioengineering, Iowa City, IA) and the resultant $I_{sc}$ recorded. Monolayers were exposed to a 5 mV bipolar pulse of 5 s duration every 100 s and the corresponding change in $I_{sc}$ was recorded. These parameters then were used to determine $R_{te}$ from Ohm's law, $R_{te} = \Delta V/\Delta I$. Data were acquired digitally at 1 Hz using an MP100A-CE interface and Aqknowledge software (ver. 3.2.6, BIOPAC Systems, Santa Barbara, CA).

*2.3.3 Immunohistochemistry*

Small portions of porcine vas deferens were snap-frozen in liquid nitrogen and then submerged in OCT embedding compound (Tissue-Tek, Sakura Finetek USA., Inc. Torrance, CA). Sections of 10 or 12 μm thickness were cut using a Leica CM3050S Cryostat. The sections were fixed in 4% paraformaldehyde (Electron Microscopy Sciences, Hatfield, PA) for 10 minutes at room temperature and rinsed with phosphate buffered saline for cytochemistry (PBS; composition in mM: 5 $KH_2PO_4$, 15 $K_2HPO_4$, and 150 NaCl, pH 7.2-7.4). To prevent non-specific binding, sections were incubated with 10% goat serum for 1 h at room temperature. Sections were then incubated with anti-KCNK5 primary antibodies (Rabbit polyclonal, Alomone Labs, Jerusalem, Israel) at 1:100 dilution in 2% normal goat serum overnight in a humid environment. Secondary antibodies were prepared by diluting Alexa Fluor 488 goat anti-rabbit IgG (Molecular Probes, Eugene, OR) in PBS containing 1% goat serum, and sections incubated for 45 minutes in the dark at room temperature. The final incubation was with TO-PRO-3 iodide (Molecular Probes) at 1:10,000 dilution for 20 minutes in the dark at room temperature. The slides were mounted with Vectashield mounting medium for fluorescence (Vector Laboratories, Burlingame, CA) and visualized using a Zeiss LSM 510 laser scanning confocal microscope.

*2.3.4 1°PVD Whole Cell Lysate Preparation*

Cell monolayers cultured on Snapwell permeable supports were used for whole cell lysate preparation. The Snapwell trays containing cells were placed on ice; media removed by aspiration and washed three times with PBS, with final wash being ice-cold PBS. RIPA buffer

(composition: 1 M TRIS-HCl pH 7.5, 1 M NaCl, 250 mM EDTA, 1% Triton-X, 1% sodium deoxycholate, and 0.1% SDS) and protease inhibitor cocktail set III (Calbiochem, La Jolla, CA) were mixed in a 1:100 ratio and added to each Snapwell permeable support (100 μL) to disrupt the cell membranes. The cells were scraped using a pipette tip, aspirated using a 22 gauge needle, transferred to a 1.5 mL eppendorf tubes and sheared by aspirating three times with a 26 gauge needle. The tubes containing lysate were placed on a rocker in a cold room for 2 hours. The lysate was then spun at 15,000 rpm at 4°C for 5 minutes and the pellet was discarded. The supernatant containing soluble protein was collected, transferred to new tubes and stored at -20°C until further use. The protein concentrations in the lysates were measured using a bicinchoninic acid assay kit (BCA; Pierce, Rockford, IL) just before performing Western blot assays.

*2.3.5 Pig Kidney Cortex Lysate Preparation*

A small amount of pig kidney was obtained from a local slaughter house and the cortex region was identified and immediately snap-frozen in liquid $N_2$ until further processing at the laboratory. About 1 g of frozen pig kidney cortex was powdered in liquid $N_2$ using mortar and pestle. 10 mL of RIPA buffer was added to the powdered tissue that was then homogenized using a polytron with one burst of 20 s duration. The homogenized mixture was then centrifuged at 15,000 rpm for 10 minutes at 4°C, supernatant collected and aliquoted into 100 μL and stored at -80°C until used. The protein concentrations in the lysates were measured using BCA just before performing Western blot assays.

*2.3.6 Western Blotting*

Protein samples were denatured by adding Laemmli sample buffer (Bio-Rad, Hercules, CA) containing sodium dodecyl sulfate (SDS) and heating at 70°C for 10 minutes. β-mercaptoethanol was added to create reducing conditions. Lysate samples (20 μg protein) were loaded in each well of 4-20% SDS-polyacrylamide gel (Bio-Rad) and resolved by electrophoresis with 30 mA for about 1 hour. Proteins were then transferred to polyvinylidene fluoride (PVDF) transfer membrane (Millipore, Bedford, MA) under semi-dry conditions at 100 mA for 3 hours. Membranes were blocked overnight at 4°C in blocking buffer containing 5% fat free dry milk (Nestle, Glendale, CA), and 0.025% sodium azide dissolved in PBS. The membranes were then probed with anti-KCNK5 antibody or anti-KCNK5 antibody pre-adsorbed with its immunizing peptide (Alomone, Jerusalem, Israel) in blocking buffer. Appropriate ECL peroxidase labeled secondary antibody was used with a digital imaging system (Image Station 4000R, Kodak, Rochester, NY).

*2.3.7 Chemicals*

Penicillin, streptomycin, amphotericin-B, collagenase, gentamicin, and trypsin-EDTA were purchased from Invitrogen (Carlsbad, CA). Forskolin was purchased from BioMol (Plymouth Meeting, PA). Bupivacaine, lidocaine, quinidine, clofilium, and riluzole were all purchased from Sigma-Aldrich (St. Louis, MO).

*2.3.8 Data Analysis*

Data are presented as means ± SE. Means were compared between treatments using a Student's *t*-test. Statistical significance was assigned at $P < 0.05$.

## 2.4 Results

*2.4.1 Apical Bupivacaine Inhibits Forskolin-Stimulated $I_{sc}$ in 1°PVD Cells*

The cultured 1°PVD cells had basal $I_{sc}$ values near zero. Forskolin exposure was employed to assess the responsiveness of the cell monolayers. The responses of 1°PVD cells to forskolin were typical (35), which was characterized by an immediate peak in $I_{sc}$ followed by a sustained plateau (see Fig. 2.1A). The increase in $I_{sc}$ was accompanied by a concurrent reduction in $R_{te}$, suggesting that a conductive pathway is activated by forskolin. It has been demonstrated previously with 1°PVD cells that an increase in $I_{sc}$ in response to forskolin is indicative of $HCO_3^-$ and/or $Cl^-$ secretion (5, 35). The sustained forskolin-stimulated $I_{sc}$ across 1°PVD cell monolayers in current studies was 4.2 ± 0.1 $\mu A/cm^2$ (n = 71). It was shown previously that pan-selective potassium channel blockers reduced forskolin-stimulated $I_{sc}$ (35). Additional experiments are required to determine the identity of channels that contribute to this response.

Bupivacaine, a local anesthetic, is known to inhibit two-pore potassium channels [TASK-2 (23) and TREK-1 (25)] in both excitable and non-excitable cells. Results presented in Fig. 2.1A demonstrate that bupivacaine (100 _M), when added to the apical bathing solution, inhibited the sustained component of $I_{sc}$ that was stimulated by forskolin. Basolateral exposure to bupivacaine also reduced forskolin-stimulated $I_{sc}$, but to a lesser extent and with slower kinetics.

Inhibition of forskolin-stimulated $I_{sc}$ by bupivacaine was concentration dependent (Fig. 2.1B). A similar pattern is observed regardless whether one examines the absolute magnitude of inhibition or the proportion of $I_{sc}$ that is inhibited. At the lowest concentration tested, 1 _M, bupivacaine caused a small, but reproducible decrease in $I_{sc}$. Incrementally greater inhibition was observed at higher concentrations with an apparent plateau being reached at 100 to 300 _M. Proportional inhibition was fitted by a modified Michalis-Menten equation, $I = I_{max}*[x/(c+x)]$, where $I$ is the proportion of $I_{sc}$ that is inhibited, $I_{max}$ is the derived maximal inhibition, x is concentration of bupivacaine, and c is the concentration of bupivacaine causing a half-maximal inhibition ($IC_{50}$). The results indicate that bupivacaine inhibits a maximum of 71.6 ± 5.8% of forskolin-stimulated $I_{sc}$, while the $IC_{50}$ was 7.4 ± 2.2 μM. The goodness of fit, as evaluated by eye and with a modified Hill equation, suggests strongly that the data are well-described by a simple bimolecular reaction scheme in which the interaction of a single bupivacaine molecule with a single transport protein (e.g., channel) results in the immediate inhibition of all dependent transport processes. Following exposure to bupivacaine, there was also a concentration-dependent increase in $R_{te}$ (Fig. 2.1C) that is consistent with the blockade of a potassium conductive pathway. The dynamic portion of the sensitivity range to bupivacaine is similar to the reported $IC_{50}$ values for inhibition of TASK-2 channels by racemic bupivacaine (26 ± 5 μM (22)), suggesting that TASK-2 inhibition by bupivacaine accounts for the reduction in $I_{sc}$ across 1°PVD monolayers.

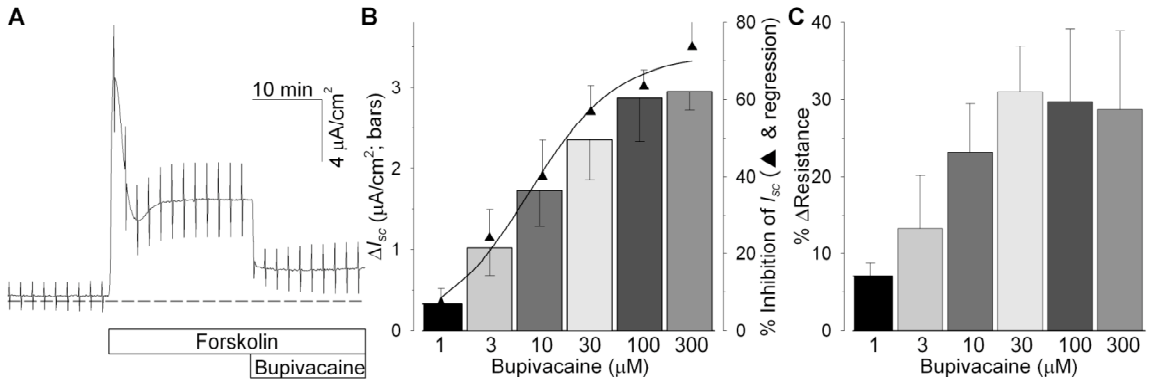


**Figure 2.1 Forskolin-stimulated $I_{sc}$ in primary porcine vas deferens epithelial cell monolayers (1°PVD cells) is inhibited by apical application of bupivacaine.**

A) Typical response of 1°PVD cells to forskolin (2 μM) and bupivacaine (100 μM apical). B) Summary of concentration-dependent inhibition of change in forskolin-stimulated $I_{sc}$ by bupivacaine in 1°PVD cells (bar graphs). Responses of 1°PVD cells to apical bupivacaine exposure are summarized as percent inhibition of forskolin stimulated $I_{sc}$. The solid line represents the best fit of a modified Michalis-Menten equation to the data set (Fit parameters reported in the text). C) Summary of percent change in trans-epithelial resistance of 1°PVD cells in response to the different concentrations of bupivacaine that were tested. Each data point represents 3-5 observations, vertical bars indicate standard error of mean (SEM).

### *2.4.2 Lidocaine, Clofilium and Quinidine Inhibit Forskolin-Stimulated $I_{sc}$ across 1°PVD Monolayers*

We sought to determine whether other putative TASK-2 blockers, when applied to the apical side of 1°PVD monolayers, had any effect on forskolin-stimulated $I_{sc}$. Lidocaine, clofilium and quinidine have been reported previously to inhibit TASK-2 and other two pore potassium channels (7, 11, 22); hence experiments were conducted to determine the effects of these pharmacological agents on forskolin-stimulated $I_{sc}$ across 1°PVD cell monolayers.

Apical application of lidocaine, similar to bupivacaine, inhibited sustained forskolin-stimulated $I_{sc}$ across 1°PVD cells (Fig. 2.2A). However, basolateral application of lidocaine had no effect. Inhibition by lidocaine was either incomplete or occurs at higher concentrations than those required for bupivacaine as the subsequent apical exposure to an equal concentration of bupivacaine (100 μM) resulted in substantially greater inhibition. Nonetheless, even over the range that was tested, inhibition of forskolin-stimulated $I_{sc}$ was concentration dependent (Fig. 2.2D). These data were replotted as percent inhibition of the forskolin-stimulated $I_{sc}$ and fitted by a modified Michalis-Menten equation that was constrained to a maximal inhibition of 71.6% (equal to $I_{max}$ derived for bupivacaine; Fig. 2.0.2E). The $IC_{50}$ for inhibition of forskolin-stimulated $I_{sc}$ by lidocaine was 531 ± 1834 μM. The concentration predicted to cause half-maximal inhibition with this analysis is slightly less than was employed in other reports to achieve TASK-2 inhibition (11, 22). Thus, the potency that is observed is in the anticipated range based upon previous reports for the inhibition of TASK-2.

Clofilium reportedly inhibits potassium currents in mTASK-2 transfected HEK293 cells with an $IC_{50}$ of 25 μM (32), although it is also known to inhibit cAMP-gated potassium channels in Calu-3 and human bronchial epithelial cells (11, 13). Apical clofilium exposure to 1°PVD monolayers caused a modest decrease in forskolin-stimulated $I_{sc}$ (Fig. 2.2B) that, like lidocaine, was superseded in magnitude by bupivacaine exposure. Inhibition by apical clofilium was clearly concentration dependent (Fig. 2.2D), although, there was not a significant change in $I_{sc}$ at the lowest concentration tested, 30 μM. Incrementally greater inhibition with 100 and 300 μM was observed in paired studies. Fitting a modified Michalis-Menten function to the data (again, with $I_{max}$ constrained to 71.6%) revealed an extremely low potency of 925 ± 12800 μM. The

tremendous variation associated with this estimate is expected, given that less than 20% inhibition was observed at the highest concentration tested, 300 μM. Basolateral exposure to clofilium also inhibited $I_{sc}$ across 1°PVD cells, although with much slower kinetics indicating that an alternative mechanism was likely affected in this approach. Rapid, concentration-dependent inhibition by apical clofilium is consistent with targeting to apical TASK-2 channels, although the concentrations required for inhibition are greater than expected. Thus, the effects of a fourth putative TASK-2 antagonist were assessed.

Quinidine has been shown to inhibit potassium currents generated by TASK-2 transfected HEK293 cells (34). Apical exposure of 1°PVD monolayers to quinidine, like bupivacaine, lidocaine, and clofilium, inhibited forskolin-stimulated $I_{sc}$ in a concentration dependent manner (Fig. 2.2D) while there was no effect of basolateral application. The $IC_{50}$ for inhibition of forskolin-stimulated $I_{sc}$ by quinidine when applied to the apical side was 274 ± 382 μM. Taken together, results presented in Figs. 2.1 and 2.2 show concentration dependent inhibition of forskolin-stimulated ion transport by four compounds that are reported to block TASK-2 channels with the following rank order of potency: bupivacaine>>quinidine>lidocaine>clofilium.

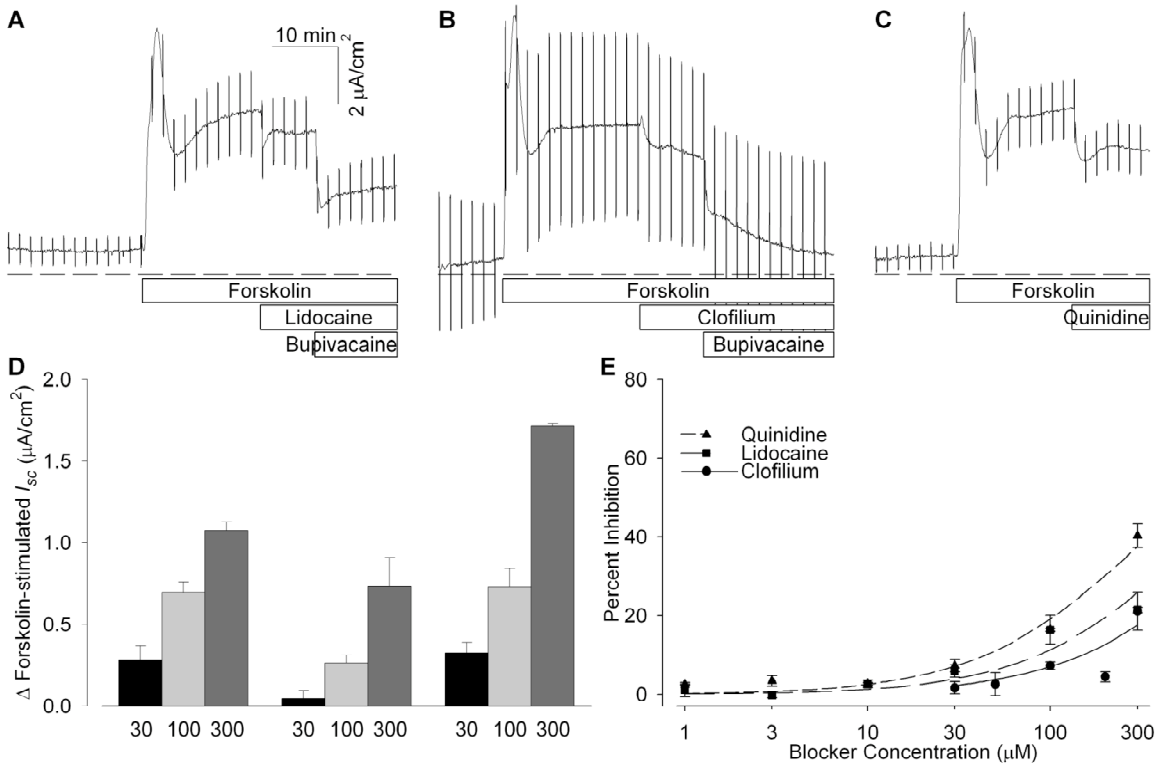


**Figure 2.2 Forskolin-stimulated $I_{sc}$ across 1°PVD cells is inhibited by apical exposure to lidocaine, clofilium or quinidine.**

Typical response of 1°PVD cells to forskolin (2 μM) and A) lidocaine (100 μM apical) followed by bupivacaine (100 μM apical), B) clofilium (100 μM apical) followed by bupivacaine, and C) quinidine (100 μM apical). D) Summary of concentration-dependent inhibition of forskolin-stimulated $I_{sc}$ by lidocaine, clofilium and quinidine across 1°PVD cell monolayers. E) Responses of 1°PVD cells to apical lidocaine, clofilium and quinidine exposure are summarized as % inhibition of forskolin-stimulated $I_{sc}$. Solid or dashed lines represent the best fit of a modified Michalis-Menten equation to each data set. Parameters of the fits are reported in the text. Data points in D and E represent 3-5 observations in each condition and vertical bars indicate standard error of mean (SEM).

*2.4.3 Riluzole, a two-pore potassium channel activator stimulates $I_{sc}$ across 1°PVD cells*

Riluzole is a neuroprotective agent used in the treatment of amyotrophic lateral sclerosis in humans that activates TREK-1 and TRAAK (15). Hence experiments were conducted to determine if riluzole had any stimulatory effect on $I_{sc}$ across 1°PVD cells. Apical exposure to riluzole (100 μM) caused a biphasic increase in $I_{sc}$. There was a transient peak in $I_{sc}$ followed by a sustained plateau (Fig. 2.3A). Basolateral application of riluzole also increased $I_{sc}$; however the response was slowly developing and small compared to the apical response (Fig. 2.3B), which might result from passive diffusion across the monolayer to affect apical channels. Results presented in Fig. 2.3C and D show that, in the presence of bupivacaine, the response to riluzole is significantly less, an outcome expected if riluzole is activating TASK-2. Thus, the pharmacology resulting from the use of five compounds, one activator and four blockers is consistent with TASK-2 activity in the apical membrane being required to achieve maximal anion secretion.

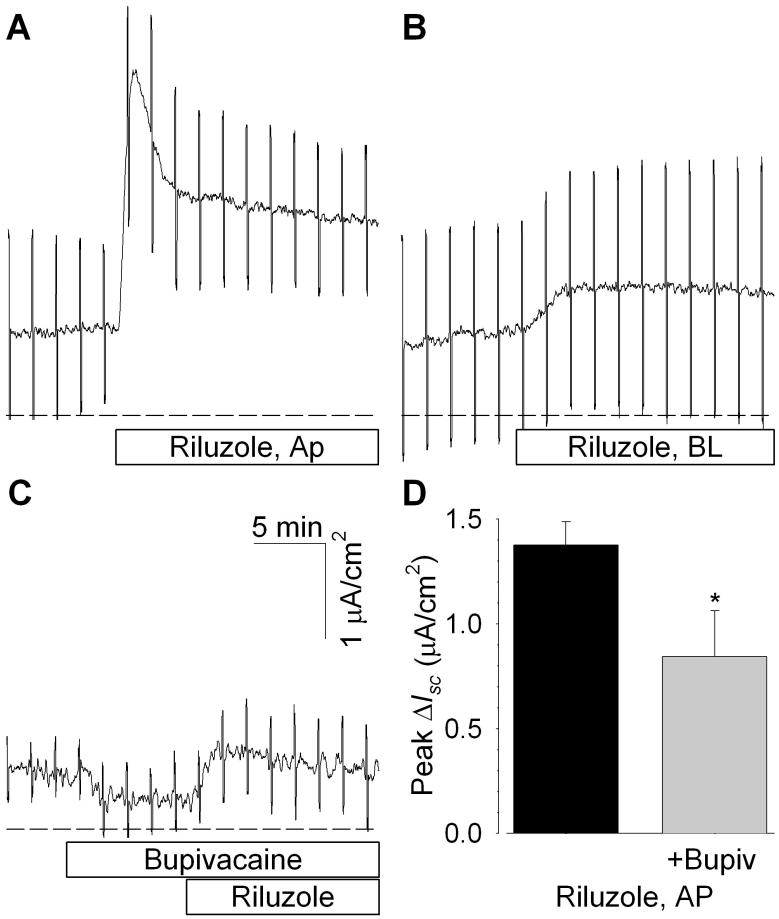


**Figure 2.3 Apical application of riluzole stimulates $I_{sc}$ across 1°PVD cells.**

Typical responses to A) apical or B) basolateral riluzole (100 μM) or C) apical riluzole in the presence of bupivacaine are shown. Results are typical of 3-5 observations per condition. D) Summary of the peak responses of 1°PVD cells to riluzole (100 μM apical) in the absence and presence of bupivacaine (100 μM apical). Results are summarized from 5 paired observations. Asterisk indicates a statistical significant difference in the responses of 1°PVD cells to riluzole alone and riluzole plus bupivacaine.

*2.4.4 1°PVD cells express TASK-2 immunoreactivity*

Antibodies raised against amino acid residues 483-499 of human TASK-2 were used to test for TASK-2 immunoreactivity in 1°PVD cell lysates. Two prominent bands were labeled

consistently at ~55 kDa by this antibody in the 1°PVD cell lysates (Fig. 2.4A) consistent with the observations made by other researchers (11, 16), whereas only single band was labeled in pig kidney cortex cell lysates (Fig. 2.4B), as expected. A band of greater mobility was also observed consistently in the 1°PVD cell lysates (Fig. 2.4A). However, when the TASK-2 antibody was pre-adsorbed with the immunizing peptide provided by the manufacturer, no labeling was observed (Fig. 2.4C and D) indicating that the immunoreactivity was likely specific to TASK-2 expressed in 1°PVD cell and pig kidney cortex lysates.

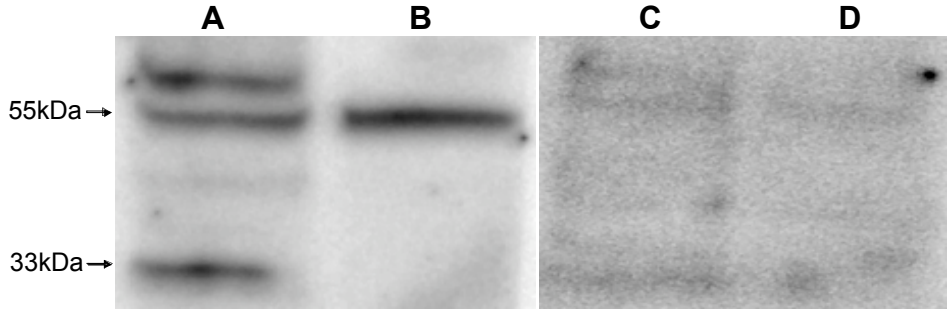


**Figure 2.4 TASK-2 immunoreactivity is present in 1°PVD cell lysates.**

1°PVD (A & C) and pig kidney cortex (B & D) cell lysates were resolved by SDS-PAGE and probed with antibodies raised against a TASK-2 epitope or the same antibodies that had been preadsorbed with the immunizing peptide (C & D). Results are typical of three separate experiments.

*2.4.5 Apical localization of TASK-2 protein in native porcine vas deferens ducts*

Experiments were conducted to determine the localization of TASK-2 in freshly procured porcine vas deferens. Tissues were processed and probed for TASK-2 immunoreactivity as described in the METHODS. Images of anti-TASK-2 labeled and TO-PRO-3 iodide stained sections of the porcine vas deferens duct were obtained as optical sections using a confocal

microscope (Fig. 2.5). A nearly continuous line of immunoreactivity is present at or near the apical membrane of cells lining the duct, suggesting that the immunoreactive epitope is present in the apical membrane of virtually all epithelial cells present in the sample. No labeling was observed either when the primary antibody was omitted from the protocol or when the primary antibody was pre-adsorbed with immunizing peptide (Fig. 2.5B & C). These results presented in Figs. 2.4 and 2.5 provide strong evidence that TASK-2 is expressed by epithelial cells lining the porcine vas deferens, which supports the observations employing pharmacological techniques to suggest that TASK-2 at the apical epithelial membrane contributes to stimulated anion secretion.

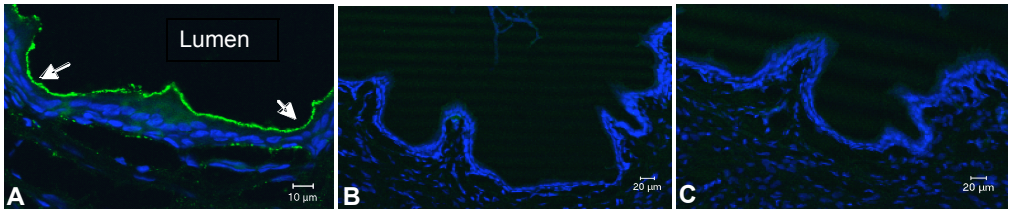


**Figure 2.5 TASK-2 immunoreactivity is present in cells lining native porcine vas deferens.**

A) TASK-2 immunoreactivity (green) is localized to the apical region of virtually all cells lining native porcine vas deferens. Immunolabeling is not observed when the primary antibody was omitted from the assay protocol (B) and is virtually absent when the primary antibody was pre-adsorbed with immunizing peptide (C). Nuclei are stained blue with TO-PRO-3 iodide. These results are typical of experiments employing vas deferens derived from three different pigs.

## 2.5 Discussion

Evidence presented in this manuscript supports a cellular model to account for vas deferens ion transport that includes a two-pore potassium channel, TASK-2, in the apical membrane of epithelial cells lining the duct. A panel of pharmacological agents including four

compounds known to block TASK-2 channels and one compound that was expected to increase TASK-2 activity had the expected effect to either reduce or enhance $I_{sc}$, respectively. Inhibition of $I_{sc}$ by each of the four blockers was concentration dependent and the rank order of potency is consistent with the expectations for inhibition of TASK-2. Immunoreactivity for TASK-2 was present in lysates derived from cultured vas deferens epithelial cells. Most importantly, antibodies raised against TASK-2 provide a robust signal at the apical membrane of virtually all epithelial cells lining the native duct. These results compel us to revise cell models that are currently envisioned to account for the generation and/or modification of the reproductive duct luminal contents by including an apical potassium conductance that contributes to the fluid and solute environment to which sperm are exposed.

Models to account for epithelial anion secretion typically include channels that provide an exit route for potassium, which enters the cell with the actions of the $Na^+/K^+$ ATPase and the $Na^+/K^+/2Cl^-$ cotransporter. Potassium exit through membrane channels concurrently hyperpolarizes the cell membrane, providing the electromotive force for anion exit at the apical membrane. Such a cellular model was proposed for epithelial cells derived from porcine vas deferens (35). Indeed, it was shown that basolateral $Ba^{2+}$ and clotrimazole, but neither charybdotoxin nor 293B, were associated with substantial inhibition of forskolin-stimulated $I_{sc}$ (35). While the published model (35) accounts for anion secretion and the observed $I_{sc}$, such a model does not account for the possibility of potassium secretion, even though the potassium concentration in luminal contents is reportedly greater than the concentration in plasma (10, 19, 26, 40). It was suggested some time ago that apical $K^+$ channels might also support anion secretion (9), and more recently it was reported that members of the two-pore potassium channel

family were expressed in the apical membrane of Calu-3 cells (11), a cell line derived from human airway that has the characteristics of serous cells. Thus, experiments were designed and conducted to test for the effects of two-pore $K^+$ channel blockers on 1°PVD ion transport.

Bupivacaine, lidocaine, clofilium and quinidine, which are known to block TASK-2 (7, 11, 22, 23), reduced forskolin-stimulated $I_{sc}$ across 1°PVD monolayers. All of these compounds inhibited forskolin-stimulated $I_{sc}$ in a concentration dependent manner when applied to the apical membrane of 1°PVD monolayers. Following the addition of all these drugs, there was also a concurrent concentration dependent increase in $R_{te}$ that is consistent with the blockade of a conductive pathway (i.e., a potassium channel). Bupivacaine was the most potent blocker with an $IC_{50}$ of <10 μM and the rank order of potency was bupivacaine>>quinidine> lidocaine>clofilium. Only bupivacaine showed an apparent maximal effect in the concentration range that was tested, inhibiting ~72% of forskolin-stimulated $I_{sc}$. These blockers were most effective when applied to the apical membrane of 1°PVD monolayers. Bupivacaine and clofilium also showed inhibitory effects with basolateral exposure although the kinetics were slower and the degree of inhibition appeared to be less, indicating that an alternative mechanism was affected. It is possible that these agents are able to partition across the epithelial monolayer to affect apical channels. Alternatively, it is possible that both an apical $K^+$ channel (in this case, TASK-2) and a basolateral bupivacaine- and clofilium-sensitive voltage gated $K^+$ channel may be activated for the electrogenic anion secretion to occur. Additionally riluzole, an activator of two-pore potassium channels (15) stimulated an increase in $I_{sc}$ when applied to the apical side of 1°PVD cells. Taken together, these data strongly suggest that functional TASK-2 $K^+$ channels are present in the apical membrane of $1^o$ PVD cells.

Western blotting revealed immunoreactivity of 1°PVD cell lysates to anti-TASK-2 antibodies and immunohistochemistry localized TASK-2 immunoreactivity to the apical side of virtually all epithelial cells lining native porcine vas deferens. Taken together, these data suggest that TASK-2 protein is present in porcine vas deferens epithelial cells and that it is functionally active and expressed at the apical side of the epithelial cells lining the duct.

Unlike other two-pore potassium channels that are predominantly expressed in excitable cells, TASK-2 is more prominently expressed in epithelial tissues such as in kidney, pancreas, liver, small intestine, lung, placenta and uterus (28, 34). In fact, it is believed to be absent from both human and mouse brain (1, 34, 41), in spite of few reports suggesting TASK-2 mRNA expression in human dorsal root ganglia and spinal cord (29) and mouse taste receptor cells (27). Nonetheless, TASK-2 has been increasingly gaining attention and is thought to play key roles in epithelial ion transport processes such as cell volume regulation in primary cultures of mouse proximal renal tubules (32), regulation of bicarbonate transport in mouse proximal renal tubules (41), vectorial chloride transport in human pancreatic duct adenocarcinoma cell line (16), $K^+$ exit/recycling across the apical membrane in Calu-3 cells (11), and in the maintenance of acid-base homeostasis (31).

Initially it was surprising that apical exposure to TASK-2 blockers was associated with a decrease in $I_{sc}$ because potassium secretion would generate a negative $I_{sc}$ and the inhibition of cation secretion would necessarily increase $I_{sc}$, opposite to what was observed. However, cells derived from porcine vas deferens, like pancreatic duct cells, express a number of bicarbonate

transporters including SLC4A4 (sodium bicarbonate cotransporter), SLC26A3, SLC26A4, SLC26A6 (chloride bicarbonate exchangers), and CFTR (chloride and bicarbonate permeant channel) (5, 6). Importantly, both SLC26A3 and SLC26A6 (36) are reportedly electrogenic, as is SLC4A4 (5). Thus, the possibility exists that the activation of TASK-2 supports bicarbonate and/or chloride exits via electrogenic exchangers.

Ion transport across porcine vas deferens epithelial cells might be modeled as shown in Fig. 2.6. CFTR and an electrogenic $Cl^-/HCO_3^-$ exchanger (e.g., SLC26A6) are present on the apical membrane along with TASK-2. The basolateral membrane includes the $Na^+/K^+$ ATPase that, in concert with an unidentified $K^+$ conductance is thought to set the resting membrane potential of the cell, a $Na^+/HCO_3^-$ cotransporter (SLC4A4), and NKCC, both of which harness the electromotive force for $Na^+$ to bring anions into the cell (5, 6, 35). It was proposed previously that exposure to forskolin or to adrenergic or adenosine receptor agonists elicit an increase in $Cl^-$ and $HCO_3^-$ secretion (4, 5, 35). Exit of $Cl^-$ through CFTR would enhance the activity of the $Cl^-/HCO_3^-$ exchanger. However, the activity of these two mechanisms, CFTR and SLC26A6 would depolarize the membrane, which would limit anion secretion.

The presence of $HCO_3^-$ in the lumen, however, would increase the activity of TASK-2, which would repolarize the cell and maintain ongoing anion secretion. As long as there is a net excess of $Cl^-$ and/or $HCO_3^-$ exit across the apical membrane relative to the amount of $K^+$ exit, the activity of TASK-2 would tend to increase $I_{sc}$. Alternatively the blockade of TASK-2 by bupivacaine would depolarize the apical membrane, reduce exit of $Cl^-$ via CFTR and reduce the driving force for the electrogenic anion exchanger, which would be seen as a decrease in $I_{sc}$.

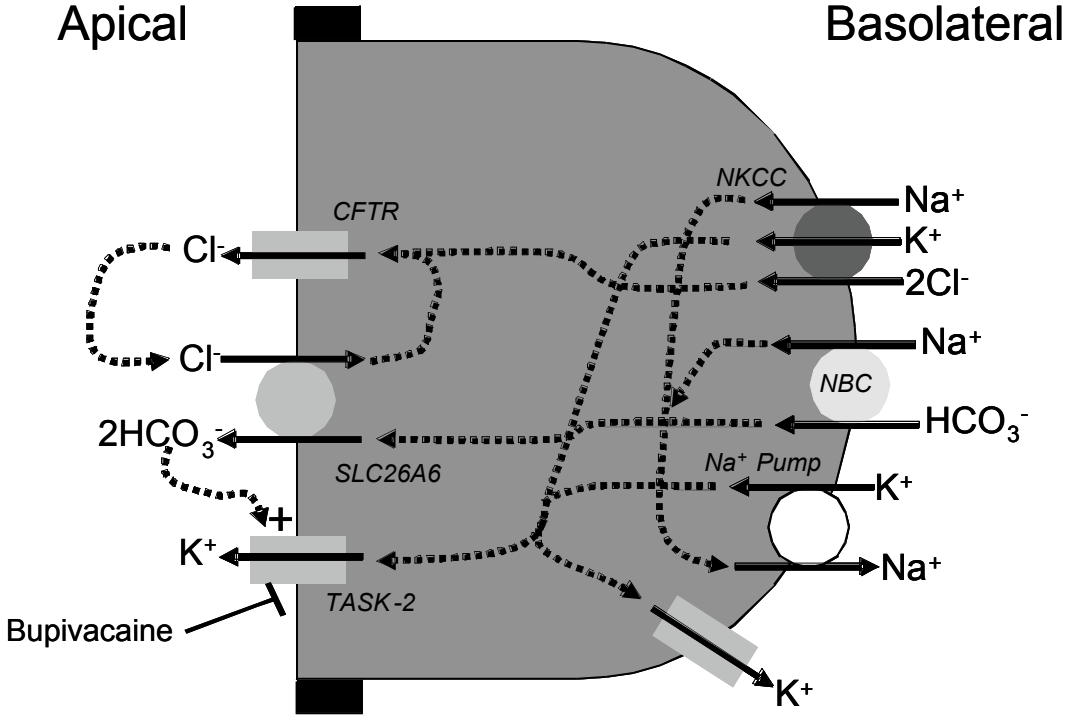


**Figure 2.6 Porcine vas deferens epithelial cell model for ion transport.**

It has been suggested that TASK-2 acts as a molecular switch for $K^+$ conductance and bicarbonate transport activity (41). In this proposed scheme, an increase in extra-cellular pH due to $HCO_3^-$ secretion activates the pH-sensitive TASK-2 to permit $K^+$ exit and thereby hyperpolarizes or repolarizes the cell membrane. This scenario can be used to explain functional significance of basolateral localization of TASK-2 in proximal renal tubule cells where there is $HCO_3^-$ reabsorption (41) and the apical localization of TASK-2 in pancreatic (16) and lung epithelial cell lines (11) where there is $HCO_3^-$ secretion. 1°PVD cells and PVD9902 cells, an epithelial cell line derived from normal porcine vas deferens, are capable of $HCO_3^-$ secretion and the results from the current study provide functional and molecular evidence for TASK-2 expression in the apical membrane of primary cultured and native porcine vas deferens epithelia,

suggesting that such a mechanism for $HCO_3^-$ associated $K^+$ secretion may be present in this tissue.

This positive feedback loop that includes TASK-2 support for $HCO_3^-$ secretion can be envisioned to have a physiological role in male fertility. Sperm are quiescent in an acid environment, which has been reported for the epididymis and vas deferens, and the sperm become active in an alkaline environment. Thus, during emotional stimulation prior to ejaculation, norepinephrine released from the hypogastric nerve would be expected to stimulate $Cl^-$ and $HCO_3^-$ secretion across vas deferens and perhaps distal epididymal epithelium. The secreted $HCO_3^-$ would activate TASK-2 to support ongoing $HCO_3^-$ secretion. Sperm in this region of the duct would initiate activity due to $HCO_3^-$ exposure. At ejaculation, the alkaline contents of the lumen would be propelled forward and the more acid contents from proximal regions of the epididymis would be propelled into this region of the duct to cause an immediate reduction in TASK-2 activity. Concurrently, norepinephrine release from the hypogastric nerve would cease and the epithelial cells would return to basal activity that includes little or no $HCO_3^-$ secretion. Any sperm in this region of the duct would be stored in a quiescent state until $HCO_3^-$ secretion is again stimulated. Thus, TASK-2 contributes to a system that modifies the luminal environment to either store sperm in a quiescent state or to activate sperm during arousal.

In conclusion, this report suggests that TASK-2 is present in the apical membrane of $1^o$PVD cells and may contribute to greater $K^+$ concentration in vas luminal fluids that may be required for maturation of sperm to occur.

## 2.6 Acknowledgements

The authors would like to thank Mr. Ryan Carlin and Drs. Rebecca Quesnell and Suma Somasekharan for technical assistance. Appreciation is also expressed to Henry's Ltd, Dr. Fernando Pierucci-Alves and Florence Wang for their assistance with tissue procurement. This project utilized the KSU-COBRE Center for Epithelial Function in Health and Disease's Confocal Microscopy and Molecular Biology Core Facilities.

## 2.7 References

1. **Aller MI, Veale EL, Linden AM, Sandu C, Schwaninger M, Evans LJ, Korpi ER, Mathie A, Wisden W, and Brickley SG.** Modifying the subunit composition of TASK channels alters the modulation of a leak conductance in cerebellar granule neurons. *J Neurosci* 25: 11455-11467, 2005.

2. **Ashmole I, Goodwin PA, and Stanfield PR.** TASK-5, a novel member of the tandem pore K+ channel family. *Pflugers Arch* 442: 828-833, 2001.

3. **Brown D and Breton S.** $H^+$V-ATPase-dependent luminal acidification in the kidney collecting duct and the epididymis/vas deferens: vesicle recycling and transcytotic pathways. *J Exp Biol* 203: 137-145, 2000.

4. **Carlin RW, Lee JH, Marcus DC, and Schultz BD.** Adenosine stimulates anion secretion across cultured and native adult human vas deferens epithelia. *Biol Reprod* 68: 1027-1034, 2003.

5. **Carlin RW, Quesnell RR, Zheng L, Mitchell KE, and Schultz BD.** Functional and molecular evidence for $Na^+$-$HCO_3^-$ cotransporter in porcine vas deferens epithelia. *Am J Physiol Cell Physiol* 283: C1033-1044, 2002.

6. **Carlin RW, Sedlacek RL, Quesnell RR, Pierucci-Alves F, Grieger DM, and Schultz BD.** PVD9902, a porcine vas deferens epithelial cell line that exhibits neurotransmitter-stimulated anion secretion and expresses numerous $HCO_3^-$ transporters. *Am J Physiol Cell Physiol* 290: C1560-1571, 2006.

7. **Cho SY, Beckett EA, Baker SA, Han I, Park KJ, Monaghan K, Ward SM, Sanders KM, and Koh SD.** A pH-sensitive potassium conductance (TASK) and its function in the murine gastrointestinal tract. *J Physiol* 565: 243-259, 2005.

8. **Clulow J, Jones RC, and Hansen LA.** Micropuncture and cannulation studies of fluid composition and transport in the ductuli efferentes testis of the rat: comparisons with the homologous metanephric proximal tubule. *Exp Physiol* 79: 915-928, 1994.

9. **Cook DI and Young JA.** Effect of $K^+$ channels in the apical plasma membrane on epithelial secretion based on secondary active $Cl^-$ transport. *J Membr Biol* 110: 139-146, 1989.

10. **Crabo B.** Studies on the Composition of Epididymal Content in Bulls and Boars. *Acta Vet Scand* 22: SUPPL 5:1-94, 1965.

11. **Davis KA and Cowley EA.** Two-pore-domain potassium channels support anion secretion from human airway Calu-3 epithelial cells. *Pflugers Arch* 451: 631-641, 2006.

12. **Decher N, Maier M, Dittrich W, Gassenhuber J, Bruggemann A, Busch AE, and Steinmeyer K.** Characterization of TASK-4, a novel member of the pH-sensitive, two-pore domain potassium channel family. *FEBS Lett* 492: 84-89, 2001.

13. **Devor DC, Bridges RJ, and Pilewski JM.** Pharmacological modulation of ion transport across wild-type and DeltaF508 CFTR-expressing human bronchial epithelia. *Am J Physiol Cell Physiol* 279: C461-479, 2000.

14. **Duprat F, Lesage F, Fink M, Reyes R, Heurteaux C, and Lazdunski M.** TASK, a human background $K^+$ channel to sense external pH variations near physiological pH. *EMBO J* 16: 5464-5471, 1997.

15. **Duprat F, Lesage F, Patel AJ, Fink M, Romey G, and Lazdunski M.** The neuroprotective agent riluzole activates the two P domain $K^+$ channels TREK-1 and TRAAK. *Mol Pharmacol* 57: 906-912, 2000.

16. **Fong P, Argent BE, Guggino WB, and Gray MA.** Characterization of vectorial chloride transport pathways in the human pancreatic duct adenocarcinoma cell line HPAF. *Am J Physiol Cell Physiol* 285: C433-445, 2003.

17. **Goldstein SA, Bayliss DA, Kim D, Lesage F, Plant LD, and Rajan S.** International Union of Pharmacology. LV. Nomenclature and molecular relationships of two-P potassium channels. *Pharmacol Rev* 57: 527-540, 2005.

18. **Hagedorn TM, Carlin RW, and Schultz BD.** Oxytocin and vasopressin stimulate anion secretion by human and porcine vas deferens epithelia. *Biol Reprod* 77: 416-424, 2007.

19. **Hinton BT, Pryor JP, Hirsh AV, and Setchell BP.** The concentration of some inorganic ions and organic compounds in the luminal fluid of the human ductus deferens. *Int J Androl* 4: 457-461, 1981.

20. **Jones RC.** Luminal composition and maturation of spermatozoa in the genital ducts of the African elephant (Loxodonta africana). *J Reprod Fertil* 60: 87-93, 1980.

21. **Kim Y, Bang H, and Kim D.** TASK-3, a new member of the tandem pore $K^+$ channel family. *J Biol Chem* 275: 9340-9347, 2000.

22. **Kindler CH, Paul M, Zou H, Liu C, Winegar BD, Gray AT, and Yost CS.** Amide local anesthetics potently inhibit the human tandem pore domain background $K^+$ channel TASK-2 (KCNK5). *J Pharmacol Exp Ther* 306: 84-92, 2003.

23. **Kindler CH, Yost CS, and Gray AT.** Local anesthetic inhibition of baseline potassium channels with two pore domains in tandem. *Anesthesiology* 90: 1092-1102, 1999.

24. **Lesage F, Guillemare E, Fink M, Duprat F, Lazdunski M, Romey G, and Barhanin J.** TWIK-1, a ubiquitous human weakly inward rectifying $K^+$ channel with a novel structure. *EMBO J* 15: 1004-1011, 1996.

25. **Lesage F and Lazdunski M.** Molecular and functional properties of two-pore-domain potassium channels. *Am J Physiol Renal Physiol* 279: F793-801, 2000.

26. **Levine N and Marsh DJ.** Micropuncture studies of the electrochemical aspects of fluid and electrolyte transport in individual seminiferous tubules, the epididymis and the vas deferens in rats. *J Physiol* 213: 557-570, 1971.

27. **Lin W, Burks CA, Hansen DR, Kinnamon SC, and Gilbertson TA.** Taste receptor cells express pH-sensitive leak $K^+$ channels. *J Neurophysiol* 92: 2909-2919, 2004.

28. **Lotshaw DP.** Biophysical, pharmacological, and functional characteristics of cloned and native mammalian two-pore domain $K^+$ channels. *Cell Biochem Biophys* 47: 209-256, 2007.

29. **Medhurst AD, Rennie G, Chapman CG, Meadows H, Duckworth MD, Kelsell RE, Gloger, II, and Pangalos MN.** Distribution analysis of human two pore domain potassium channels in tissues of the central nervous system and periphery. *Brain Res Mol Brain Res* 86: 101-114, 2001.

30. **Miller C.** An overview of the potassium channel family. *Genome Biol* 1: REVIEWS0004, 2000.

31. **Morton MJ, Abohamed A, Sivaprasadarao A, and Hunter M.** pH sensing in the two-pore domain $K^+$ channel, TASK2. *Proc Natl Acad Sci U S A* 102: 16102-16106, 2005.

32. **Niemeyer MI, Cid LP, Barros LF, and Sepulveda FV.** Modulation of the two-pore domain acid-sensitive $K^+$ channel TASK-2 (KCNK5) by changes in cell volume. *J Biol Chem* 276: 43166-43174, 2001.

33. **Pierucci-Alves F and Schultz BD.** Bradykinin-stimulated cyclooxygenase activity stimulates vas deferens epithelial anion secretion in vitro in swine and humans. *Biol Reprod* 79: 501-509, 2008.

34. **Reyes R, Duprat F, Lesage F, Fink M, Salinas M, Farman N, and Lazdunski M.** Cloning and expression of a novel pH-sensitive two pore domain $K^+$ channel from human kidney. *J Biol Chem* 273: 30863-30869, 1998.

35. **Sedlacek RL, Carlin RW, Singh AK, and Schultz BD.** Neurotransmitter-stimulated ion transport by cultured porcine vas deferens epithelium. *Am J Physiol Renal Physiol* 281: F557-570, 2001.

36. **Shcheynikov N, Yang D, Wang Y, Zeng W, Karniski LP, So I, Wall SM, and Muallem S.** The Slc26a4 transporter functions as an electroneutral $Cl^-/I^-/HCO_3^-$ exchanger: role of Slc26a4 and Slc26a6 in $I^-$ and $HCO_3^-$ secretion and in regulation of CFTR in the parotid duct. *J Physiol* 586: 3813-3824, 2008.

37. **Silva P, Stoff J, Field M, Fine L, Forrest JN, and Epstein FH.** Mechanism of active chloride secretion by shark rectal gland: role of $Na^+$-$K^+$-ATPase in chloride transport. *Am J Physiol* 233: F298-306, 1977.

38. **Sohma Y, Harris A, Wardle CJ, Gray MA, and Argent BE.** Maxi $K^+$ channels on human vas deferens epithelial cells. *J Membr Biol* 141: 69-82, 1994.

39. **Tan YP and Young JA.** Effect of $K^+$ channels in the luminal membrane of lacrimal acinar cells. *J Membr Biol* 89: 139-146, 1989.

40. **Turner TT, Hartmann PK, and Howards SS.** In vivo sodium, potassium, and sperm concentrations in the rat epididymis. *Fertil Steril* 28: 191-194, 1977.

41. **Warth R, Barriere H, Meneton P, Bloch M, Thomas J, Tauc M, Heitzmann D, Romeo E, Verrey F, Mengual R, Guy N, Bendahhou S, Lesage F, Poujeol P, and Barhanin J.** Proximal renal tubular acidosis in TASK2 $K^+$ channel-deficient mice reveals a mechanism for stabilizing bicarbonate transport. *Proc Natl Acad Sci U S A* 101: 8215-8220, 2004.

42. **Wong PY and Lee WM.** Potassium movement during sodium-induced motility initiation in the rat caudal epididymal spermatozoa. *Biol Reprod* 28: 206-212, 1983.

43. **Wong PY and Yeung CH.** Absorptive and secretory functions of the perfused rat cauda epididymidis. *J Physiol* 275: 13-26, 1978.

# CHAPTER 3 - Potential experiments and future directions

## 3.1 Overview

The results presented in Chapter 2 certainly support the contention that TASK-2 is present in the apical membrane of epithelial cells lining porcine vas deferens. However, these results are not unequivocal. None of the pharmacological agents employed are specific (or even highly selective) for TASK-2. Thus one or more alternative $K^+$ channels may have been targeted by these agents over the concentration ranges tested. For example, 100 μM quinidine has been reported to inhibit TWIK-1 and TREK-1 in addition to TASK-2. Also, the $IC_{50}$ for inhibition of voltage-gated $Na^+$ channels in HEK293 cells by bupivacaine is in the same range (4.5 μM; Wang *et al*, 2001) as seen in our inhibition of forskolin-stimulated $I_{sc}$ by bupivacaine in porcine vas deferens epithelial cells (7.4 μM, see Results, Chapter 2). Likewise, Western blots and immunohistochemistry provide evidence that the epitope derived from TASK-2 is present at the apical membrane of these epithelial cells. However, there is the possibility that this epitope is present in another protein and there is the possibility that protein carrying this epitope, regardless of its identity, is not integrated into the apical membrane. Thus, additional lines of evidence could be generated to test the hypothesis that TASK-2 is present in porcine vas deferens epithelial cell apical membranes and contributes to net anion secretion.

Gene microarray of RNA isolated from porcine vas deferens epithelial cells can be used to examine the expression of various $K^+$ channel genes. Such $K^+$ channel candidates can then be selected for subsequent RT-PCR analyses to confirm the presence of full length mRNA transcripts and to determine relative abundance of each coding message. Presence of mRNA however, does not confirm the presence of proteins or that those gene products contribute to net ion transport. Rather, the presence of mRNA provides evidence that the message is in place to synthesize TASK-2 or other $K_{2P}$ channels.

Immunoreactivity is employed to implicate the expression of an epitope that is unique to a protein of interest. Indeed, results presented in Fig. 2.4 demonstrate that a protein of the expected mobility is labeled by an antibody raised against a TASK-2 epitope. To bolster the veracity of these data, additional Western blotting can be performed using antibodies that are raised against epitopes derived from both N- and C-termini of TASK-2. Lysates from porcine kidney cortex can be analyzed in parallel since TASK-2 expression has been reported routinely for the kidney. The kidney lysate samples would be expected to reveal a single band of expected mobility with each antibody for comparison to the vas deferens cell lysates (as shown in Fig. 2.4). To confirm the identity of the TASK-2 protein in these cells, the porcine vas deferens epithelial cell lysate can be immunoprecipitated with anti-TASK-2 antibody, resolved by SDS-PAGE, visualized by Coomassie blue, excised at the expected mobility and analyzed using Matrix-Assisted Laser Desorption/Ionization Time of Flight (MALDI-TOF) mass spectrometry to confirm the protein identity. Results from these experiments will provide an unequivocal line of evidence for TASK-2 protein expression in porcine vas deferens epithelial cells.

Whether this TASK-2 protein is located at apical, basolateral or both surfaces is of crucial physiological importance in porcine vas deferens epithelial cells. In order to determine this localization, immunofluorescence using confocal microscopy was employed, which revealed labeling by anti-TASK-2 antibodies of virtually all the cells lining the lumen of a freshly frozen porcine vas deferens (Fig. 2.5). However, it can not be ascertained from this technique whether the immunolabeling observed is in the apical cell membrane, or in the sub-apical vesicles of the cells lining the lumen of vas deferens. Apical membrane incorporation can be verified by performing cell-surface biotinylation wherein biotin is conjugated to the apical or basolateral cell surface proteins without altering their biological activity and then detecting that labeled protein by Western blotting with anti-TASK-2 antibody using avidin.

Functional studies can be conducted to test for TASK-2 activity in the apical membrane of the porcine vas deferens epithelial cells. TASK-2 channels are sensitive to changes in extracellular pH with maximal activity reported at pH 8.8 and progressively less current as pH was decreased (Warth *et al*, 2004). In the current context, forskolin-stimulated $I_{sc}$ can be measured in 1°PVD cells that are maintained in normal physiological salt solutions that are buffered to selected pH values ranging from 5.4 to 9.4. The experiment can be conducted in two different ways. One way is to measure the magnitude of forskolin-stimulated $I_{sc}$ in 1°PVD cells that are bathed on the basolateral side with HEPES buffered saline (pH 7.4) and on the apical side with different buffer solutions having pH values of 5.4 (citrate buffer), 6.4 (MOPS buffer), 7.4 (HEPES buffer), 8.4 (Tris buffer), and 9.4 (borate buffer). If TASK-2 is rate limiting for ion transport, the expectation is that the greatest response to forskolin will be observed in the chamber that is exposed to apical pH of 8.4 or 9.4. A further test of this hypothesis would

include apical exposure to bupivacaine (100 μM) with the expectation that the magnitude of the bupivacaine-sensitive current would be greatest at pH 8.4 or 9.4 and that there would be no bupivacaine-sensitive current at pH 5.4. An alternative, although more difficult, approach to test for pH sensitivity in the response to forskolin is to place the monolayers at symmetrical pH of 7.4, expose the cells to forskolin to maximize $I_{sc}$, and then adjust the apical pH either up or down in the absence or presence of apical bupivacaine. If TASK-2 is involved in the response, the expectation would be that the magnitude of $I_{sc}$ would increase as pH was increased and decrease as the pH was lowered, but only in the monolayers not exposed to bupivacaine. While there may be other concerns regarding the practical implementation of these experiments that must be addressed concurrently (e.g., is pH 5.4 or 9.4 detrimental to the cell monolayers), the outcomes will provide strong evidence to either exclude or incorporate TASK-2 in the epithelial apical membrane as depicted in Fig. 2.6.

An alternative method to implicate the presence of TASK-2 in the apical membrane of 1°PVD cells is to test for bupivacaine-sensitive $K^+$-dependent $I_{sc}$ across isolated apical membranes. These experiments are conducted by establishing an apical to basolateral gradient in the concentration of $K^+$ (replace apical $Na^+$ with $K^+$) and permeabilizing the basolateral membrane with nystatin. TASK-2 activity could be maximized by employing an apical pH of 8.4 and exposing the monolayer to forskolin. If TASK-2 is present and active in the apical membrane, the $I_{sc}$ should be positive, indicating net cation absorption and the $I_{sc}$ should be reduced substantially by bupivacaine. Since there is no gradient for $Cl^-$ secretion in this arrangement and since the $Na^+$ concentration gradient would tend to decrease $I_{sc}$, the expected results would rule out the possibilities that bupivacaine is having the affect on intact tissues by

inhibiting either $Na^+$ or $Cl^-$ channels. The expected outcome would support the conclusion that TASK-2 is actually integrated into the apical membrane and contributes to the observed $I_{sc}$.

So, are TASK-2 channels required to observe a maximal $I_{sc}$ response to forskolin? One way to answer this question is by reducing or eliminating TASK-2 expression using RNA interference (RNAi). It has been reported that TASK-2 protein expression and current were significantly down regulated in TASK-2 stably transfected HEK293 cells following the incorporation of small interfering RNA (siRNA) against TASK-2 (Gonczi *et al*, 2006). The effectiveness of RNAi can be determined at the mRNA and protein levels by RT-PCR and Western blotting, respectively. Any difference in the magnitude of forskolin-stimulated $I_{sc}$ response between control 1°PVD cells and 1°PVD cells transfected with siRNA against TASK-2 can be suggestive of a role for TASK-2 channels in anion secretion. In 1°PVD cells treated with TASK-2 siRNA, forskolin would be expected to stimulate some, albeit reduced, level of $I_{sc}$. However, this response would be expected to be insensitive to either changes in apical pH or to bupivacaine. Such an outcome would provide the most compelling evidence that TASK-2 is required for maximal ion transport across vas deferens epithelial cells.

In conclusion, a cellular model that incorporates TASK-2 in the apical membrane is presented in Fig. 2.6 and evidence supporting this model is presented throughout chapter 2. Each figure provided evidence that was supportive of the model, but in isolation was not compelling. The combination of techniques, however, provides a body of evidence that is substantive, but neither exhaustive nor definitive. Thus, additional techniques and reagents as outlined in the current chapter can be used to test the model presented in Fig. 2.6 further. Each of the suggested

experiments tests a distinct hypothesis regarding the expression and function of TASK-2. Some or all of these techniques will likely be required to provide evidence that is viewed as compelling by many scientists in this field.

## 3.2 References

Gonczi M, Szentandrassy N, Johnson IT, Heagerty AM, and Weston AH. Investigation of the role of TASK-2 channels in rat pulmonary arteries; pharmacological and functional studies following RNA interference procedures. Br J Pharmacol 147: 496-505, 2006.

Warth R, Barriere H, Meneton P, Bloch M, Thomas J, Tauc M, Heitzmann D, Romeo E, Verrey F, Mengual R, Guy N, Bendahhou S, Lesage F, Poujeol P, and Barhanin J. Proximal renal tubular acidosis in TASK2 $K^+$ channel-deficient mice reveals a mechanism for stabilizing bicarbonate transport. Proc Natl Acad Sci U S A 101: 8215-8220, 2004.